# Quasiclassical description of interband magneto-optical transitions in quantum wells

A. Yu. Dobin and V. I. Perel'

*A. F. Ioffe Physicotechnical Institute, Russian Academy of Sciences, 194021 St. Petersburg, Russia*
(Submitted 5 January 1996)
Zh. Éksp. Teor. Fiz. **110**, 270–286 (July 1996)

The selection rules and expressions for the matrix elements of transitions are obtained in the semiclassical approximation for cubic semiconductors with consideration of the real band structure. The results are expressed in terms of the wave functions in a quantum well without a magnetic field and the characteristics of the classical motion of the particles in orbits in a magnetic field. It is shown that the intensity of a transition is the result of the interference of the fields of the emitting dipoles corresponding to the crossing points of the electron and hole orbits.
 [S1063-7761(96)02007-0]

## 1. INTRODUCTION

Magneto-optical transitions in quantum wells have been actively studied in recent years.[1] The hole wave functions and the transition matrix elements are usually calculated numerically for the lowest Landau levels[2–4] and, as a rule, in the cylindrical approximation. The warping of the valence band was taken into account in a calculation of the hole spectrum in a quantum well in Ref. 5 and in a calculation of the optical transitions in the bulk in Ref. 6. The purpose of the present work is a semiclassical treatment of interband magneto-optical transitions. Such a treatment will enable us to express the wave functions and transition matrix elements in a magnetic field in terms of the corresponding quantities in the absence of a magnetic field. It would then be possible to take into account features associated with the real band structure and the symmetry of a quantum well. We note that hole states in a magnetic field were previously treated semiclassically for the bulk case[7] and in the spherical approximation for a quantum well.[1)]

From a semiclassical point of view, optical transitions occur at the crossing points of electron and warped hole orbits with coinciding centers. An oscillating dipole is associated with each such crossing point. The interference of the fields of these dipoles shapes the intensity of each transition and leads to selection rules. The relative phases of the dipoles are determined by the geometric characteristics of the orbits, which, in turn, are related to the symmetry of the crystal.

The overall symmetry properties of the wave functions of electrons and holes in a quantum well without a magnetic field are described in the Appendix. The following types of symmetry are considered: $O_h$ and $T_d$ symmetry for the bulk material in a symmetric quantum well ($O_hS$ and $T_dS$), as well as in an asymmetric well ($O_hA$ and $T_dA$). In addition, the frequently employed cylindrical approximation, i.e., $CS$ and $CA$ symmetry, is also considered. This approximation is, in fact, realized in a quantum well (in contrast to the bulk case) at small values of the hole kinetic energy(compared with the size-quantized energy).

In Sec. 2 the wave functions of electrons at the Landau levels in the valence and conduction bands are expressed in terms of the wave functions and the spectrum in a quantum well without a magnetic field, as well as in terms of the characteristics of the classical motion of the particles in orbits in a magnetic field. We note that the classification of the states at the Landau levels in the valence band is ambiguous. The numbering chosen in the present work seems most natural to us. For a specific size-quantized subband, two states correspond to each Landau level number. Under $O_hS$ symmetry one of these states is symmetric, and the other is antisymmetric with respect to the reflection $\hat{\Pi}_z$, and they have opposite magnetic moments.

In Sec. 3 semiclassical expressions are obtained for the matrix elements of magneto-optical transitions. Selection rules are derived for each of the types of symmetry enumerated above. The selection rules for $CS$ and $CA$ symmetry can be interpreted as an angular momentum conservation law. Under $O_hS$, $T_dS$, and $O_hA$ symmetry the angular momentum is maintained with an accuracy to $4N$ ($N$ is an integer). In all these cases the transitions are circularly polarized. Under $T_dA$ symmetry there is an additional axis in the plane of the well, and the transitions are elliptically polarized.

The results of numerical calculations for a rectangular well with infinitely high barriers based on GaAs in the approximation of $O_hS$ symmetry are presented as an example.

It is assumed in this work that the well points in the [001] direction, and that the magnetic field and the light ray are perpendicular to the plane of the well (this Faraday geometry). The Coulomb interaction between an electron and a hole is neglected.

## 2. WAVE FUNCTIONS OF ELECTRONS IN A MAGNETIC FIELD

The wave functions of valence-band electrons can be written in the form

$$\Psi=\sum_{\mu}\psi_{\mu}u_{\mu}. \tag{1}$$

Here the $u_{\mu}$ are the Bloch amplitudes at the top of the valence band [see (A5)], and the $\psi_n$ are the envelopes, which satisfy the following equation with an effective matrix Hamiltonian:

$$\{\hat{\mathscr{H}}(z,\hat{\mathbf{k}})-\mathbf{H}\hat{\mathbf{M}}_l\}\hat{\psi}=E\hat{\psi}, \tag{2}$$

 1063-7761/96/070146-09$10.00  

where $\hat{\mathscr{H}}$ is a matrix that depends on the operators $\hbar\hat{\mathbf{k}}=-i\hbar\nabla-(e/c)\mathbf{A}$ ($\hat{\mathbf{k}}$ is a two-dimensional vector in the plane of the well, and $e=-|e|$ is the electron charge) and is an operator with respect to the variable $z$, $\hat{\mathbf{M}}_1$ is a matrix that describes the direct interaction of the intrinsic magnetic moment of the electron with the magnetic field, and $\hat{\psi}$ is a column vector with components $\psi_\mu$. In accordance with the semiclassical method we write $\hat{\psi}$ in the form

$$\hat{\psi}=\exp[iS/\hbar]\hat{\chi}. \tag{3}$$

Then in the zeroth approximation with respect to $\hbar$ we obtain the system of equations (it is assumed that $\hat{\mathbf{M}}_1$ is first-order with respect to $\hbar$)

$$\hat{\mathscr{H}}(z,\mathbf{k})\hat{\chi}=E\hat{\chi}, \tag{4}$$

where $\hbar\mathbf{k}=\nabla S-(e/c)\mathbf{A}$.

Equation (4) is the equation for the envelopes of the wave functions of an electron in the valence band in the absence of a magnetic field. In the case of $O_hS$ or $CS$ symmetry, it has two solutions: $\chi_\mu^{(m)}(z,\mathbf{k})$ and $\chi_\mu^{(-m)}(z,\mathbf{k})$, which correspond to the same energy $E=\varepsilon(\mathbf{k})$. The properties of these solutions are considered in the Appendix. To be specific, we assume that the solution $\chi_\mu^{(m)}(z,\mathbf{k})$ is symmetric and that $\chi_\mu^{(-m)}(z,\mathbf{k})$ is, therefore, antisymmetric with respect to the reflection $\hat{\Pi}_z$ (the value of $|m|$ is fixed by the type of the size-quantized subband: $|m|=3/2$ for heavy-hole subbands and $|m|=1/2$ for light-hole subbands).

In analogy to Ref. 7 we can write

$$\chi_\mu=\sigma^{-1/2}[b_m\hat{\chi}^{(m)}+b_{-m}\hat{\chi}^{(-m)}], \tag{5}$$

where $\sigma$ is the Jacobian for the transformation from Cartesian to radial coordinates, and the $b_{\pm m}$ satisfy the transfer equations

$$i\hbar\frac{db_\alpha}{dt}=-H\sum_\beta M^{\alpha\beta}b_\beta,$$

$$M^{\alpha\beta}=\int dz\sum_{\mu,\mu'}\chi_\mu^{(\alpha)*}\hat{M}_{\mu\mu'}\chi_{\mu'}^{(\beta)}, \tag{6}$$

in which $\alpha$ and $\beta$ run through the values of $m$ and $-m$ (the value of $|m|$ is fixed) and $\hat{M}_{\mu\mu'}$ is the magnetic moment matrix operator:

$$\hat{M}=\frac{-ie}{2c}\left[(\hat{\mathbf{V}}+\mathbf{v})\frac{\partial}{\partial\mathbf{k}}\right]_z+\hat{M}_{1z},$$

$$\hat{\mathbf{V}}=\frac{1}{\hbar}\frac{\partial\hat{\mathscr{H}}(z,\mathbf{k})}{\partial\mathbf{k}},\quad \mathbf{v}=\frac{1}{\hbar}\frac{\partial\varepsilon(\mathbf{k})}{\partial\mathbf{k}}. \tag{7}$$

In deriving Eqs. (6) we introduced the time on the trajectory, $t$, on which the kinematic momentum vector $\mathbf{k}$ depends: $\hbar d\mathbf{k}/dt=(e/c)(\mathbf{v}\times\mathbf{H})$.

It can be shown that the off-diagonal elements of the matrix $M^{\alpha\beta}$ are equal to zero, i.e., $M^{m,-m}=M^{-m,m}=0$, because $\hat{\chi}^{(m)}$ and $\hat{\chi}^{(-m)}$ have different symmetries under the reflection $\hat{\Pi}_z$. Therefore, the system (6) decomposes into two independent equations for $b_m$ and $b_{-m}$, each of which can easily be solved. The value $b_{-m}=0$ can be chosen for one of the solutions, and $b_m=0$ can be chosen for the other solution, and the wave functions $\Psi$ in the magnetic field can be characterized by $m$ or $(-m)$, respectively. Then the function $\Psi^{(m)}$ is symmetric, and $\Psi^{(-m)}$ is antisymmetric under the reflection $\hat{\Pi}_z$.

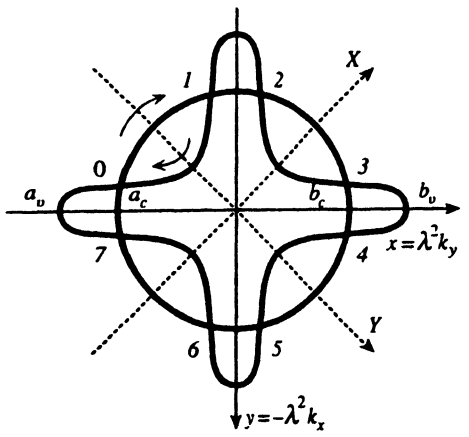


FIG. 1. Trajectories of the valence-band and conduction-band electrons. The centers of the orbits are located at the point $x=y=0$. The crossing points of the orbits are numbered (just like the corresponding sectors in the $\mathbf{k}$ plane; see the Appendix). The arrows indicate the direction of motion of particles in the orbits.

To be specific, we now introduce the Landau gauge in the coordinates $x$ and $y$ (see Fig. 1): $A_x=0$, $A_y=Hx$. The $x$ and $y$ axes are turned through a $\pi/4$ angle relative to the $X$ and $Y$ crystal axes, as is shown in Fig. 1. This choice of coordinate system was dictated by the shape of the hole orbits. The action is written in the form $S=\hbar qy+\hbar s(x)$, $q=\text{const}$ is an integral of the motion,

$$\hbar k_x=\frac{\partial S}{\partial x},\quad \hbar k_y=\hbar q-\frac{e}{c}Hx=-\frac{e}{c}H(x-x_0),$$

$$x_0=\frac{\hbar c}{eH}q. \tag{8}$$

This choice of gauge corresponds to a family of trajectories having centers with the coordinates $(x_0,y_0)$. We assumed that $x_0=\text{const}$ and that the trajectories in the family have different values of $y_0$, which constitutes the second radial coordinate (besides $t$). In this case $\sigma=|v_x|$.

The equation $E=\varepsilon(\mathbf{k})$ defines $k_x$ as a function of $k_y$, and therefore of $x$, according to (8). At each point $x$ there are two solutions of this equation for $k_x$ that differ in sign. (The $x,y$ coordinate system, rather than the $X,Y$ system, was chosen specifically because in this system the equation $E=\varepsilon(\mathbf{k})=\text{const}$ has two and only two solutions of $k_x$ at a given $k_y$ for a real band structure.)

In accordance with the Keller–Rubinov method,[8] the true wave function is a sum of functions corresponding to two leaves, on one of which $k_x>0$, while on the other $k_x<0$. Thus, the components of the wave function of the valence-band electrons in a quantum well in a magnetic field have the form

$$\psi_\mu = \exp(iqy)\sqrt{\frac{\omega}{2\pi|v_x|}}\left\{\exp[i\theta(x)]\chi_\mu(z,\mathbf{k}) + \exp\left[-i\theta(x)+\frac{i\pi}{2}\right]\chi_\mu^*(z,Q_6\mathbf{k})\right\}. \quad (9)$$

Here the normalization length is assumed to be equal to unity, $\omega$ is the cyclotron frequency, $\hbar\mathbf{k}$ is the momentum of the electron in the classical orbit at the point $x$,

$$\theta(x)=s(x)+m(x), \quad s(x)=\int_a^x k_x dx,$$

$$m(x)=\hbar^{-1}\int_0^{t(x)} HMdt. \quad (10)$$

In writing Eq. (9), we took advantage of the fact that in the second leaf $\theta(x)$ changes sign and that the function $\hat{\chi}_\mu^{(m)}$ in the second leaf can be obtained using the operator $\hat{Q}_6^{(m)}$ [see (A7)]. The point $a$ is the left-hand turning point, and $t(x)$ is the time of motion from $a$ to $x$. It was taken into account that upon passage from the first to the second leaf (passage through a caustic), a phase of $\pi/2$ is acquired, and a normalization factor is introduced.[9] In (10) $M$ denotes the diagonal element of the matrix $M^{\alpha\beta}$ from (6). The index $m$ (or $-m$) is omitted everywhere for the sake of brevity.

The quantization conditions have the form

$$2\theta(b)-\pi=2\pi n, \quad (11)$$

where $b$ is the right-hand turning point. If we introduce the area $A$ of the orbit in the $\mathbf{k}$ plane and the magnetic moment

$$\mu=\frac{1}{T}\int_0^T Mdt \quad (12)$$

[$T$ is the orbital period, and $t(b)=-T/2$ for the valence-band electrons] into the discussion, (12) can be rewritten in the form

$$\lambda^2 A=2\pi\left(n+\frac{1}{2}-\frac{\mu H}{-\hbar\omega}\right), \quad (13)$$

where $\lambda$ is the magnetic length. We stress that by virtue of (A10), the values of $M$ and, therefore, the magnetic moment $\mu$ differ in sign for the states $\Psi^{(m)}$ and $\Psi^{(-m)}$ belonging to the same Landau level.

Let us now consider the changes caused by lowering of the symmetry due to the lack of an inversion center ($T_d$ symmetry for the bulk material or asymmetry of the quantum well). We assumed that the Hamiltonian in Eq. (2) can be written in the form $\hat{\mathscr{H}}(z,\hat{\mathbf{k}})=\hat{\mathscr{H}}_0(z,\hat{\mathbf{k}})+\hat{\mathscr{V}}(z,\hat{\mathbf{k}})$, where $\hat{\mathscr{H}}_0(z,\hat{\mathbf{k}})$ is the Hamiltonian in the approximation of $O_hS$ symmetry, and the perturbation $\hat{\mathscr{V}}(z,\hat{\mathbf{k}})$ is due to the absence of the inversion center. We first assume that this perturbation is small. Then in the zeroth approximation we can write $\hat{\mathscr{H}}_0(z,\hat{\mathbf{k}})\hat{\chi}=E\hat{\chi}$ instead of Eq. (4), and we can include $\hat{\mathscr{V}}(z,\hat{\mathbf{k}})$ in the transfer equation along with $(-H\hat{M}_{1z})$. For $\hat{\chi}$ we obtain Eq. (5), in which $\hat{\chi}^{(m)}$ and $\hat{\chi}^{(-m)}$ are eigenfunctions of the Hamiltonian $\hat{\mathscr{H}}_0(z,\hat{\mathbf{k}})$ that are assigned to the same energy $E=\varepsilon_0(\mathbf{k})$. In Eq. (3) for $\hat{\psi}$ it must be borne in mind that the action $S$ is determined by the energy $\varepsilon_0(\mathbf{k})$.

The modified transfer equations will have the form (6) with replacement of the matrix $(-HM^{\alpha\beta})$ by the matrix $G^{\alpha\beta}=-HM^{\alpha\beta}+U^{\alpha\beta}$. In these equations the terms $\hbar db/dt$ and $HMb$ are of order $\hbar\omega b$ ($\hbar\omega$ is the distance between neighboring Landau levels), and the term $Ub$ is of order $\Delta\varepsilon b$, where $\Delta\varepsilon$ is the splitting between the two branches of the size-quantized subbands (without a magnetic field) caused by the lack of an inversion center. When $\hbar\omega\gg\Delta\varepsilon$, we can neglect the term $Ub$ in the modified transfer equations, and we wind up with the case of $O_hS$ (or $CS$) symmetry considered above. Thus, even when there is no inversion center, in a sufficiently strong magnetic field the states can be considered nearly symmetric or antisymmetric under the reflection $\hat{\Pi}_z$. As the magnetic field weakens, we go over to the situation $\hbar\omega\ll\Delta\varepsilon$, in which the two branches assigned to one size-quantized subband are quantized in the magnetic field independently of one another.

We shall not dwell on the solution of the modified transfer equations in this limiting case. Instead, we at once [without assuming that the perturbation $\hat{\mathscr{V}}(z,\hat{\mathbf{k}})$ is small] consider Eq. (4), assuming that it has a unique solution for each of the two nondegenerate (when $k\neq 0$) branches of the size-quantized subband. Now, instead of the system (6) we have one transfer equation for each of the branches. Equations (7)–(13) remain in force as before. The quantization conditions (13) give two independent Landau ladders, which are shifted along the energy scale relative to one another by an amount of order $\Delta\varepsilon\gg\hbar\omega$.

We focus our attention on one significant circumstance. The wave functions $\Psi_\mathbf{k}$ in the absence of a magnetic field, which are used to construct the semiclassical states in a magnetic field, can contain an arbitrary phase factor that depends on $\mathbf{k}$. The choice of this phase factor cannot, of course, alter the physical results. In fact, according to (7), the multiplication of $\hat{\chi}$ by the phase factor $\exp[i\beta(\mathbf{k})]$ leads to the addition of $(-d\beta/dt)$ to $HM/\hbar$. As a result $\hat{\psi}$ acquires only the constant phase factor $\exp[i\beta_0]$, where $\beta_0$ is the value of $\beta(\mathbf{k})$ at $t=0$. However, variation of the phase factor alters the magnetic moment $\mu$ and the numbering of the Landau levels. More specifically, if the phase $\beta(\mathbf{k})$ acquires an increment $2\pi N$ (where $N$ is an integer) during a complete period, the magnetic moment $\mu$ [according to (12)] acquires the term $(-N\hbar\omega/H)$, which corresponds to a change in the level number $n$ [under the quantization conditions (13)] by $n+N$.

It can be shown that by assigning the indices $m$ to the states [i.e., by assigning transformation laws using the operators $\hat{Q}_n^{(m)}$ or $\bar{Q}_n^{(m)}$], we fix the increment of the phase of the wave function in a complete period to an accuracy of $2\pi\cdot 4N$ ($N$ is an integer). Thus, the magnetic moment $\mu$ is fixed to an accuracy of $4N\hbar\omega/H$, and, therefore, the Landau-level number is fixed to an accuracy of $4N$.

Under $O_hS$ (or $CS$) symmetry the assignment of the indices $m$ and $-m$ to states having the same Landau-level number leads to the usual scheme of Landau levels split by $\pm\mu H$. In cases of lower symmetry this scheme is maintained approximately, if the magnetic field is strong enough for $\hbar\omega$ to be greater than the splitting between the two branches of the spectrum in the absence of a magnetic field.

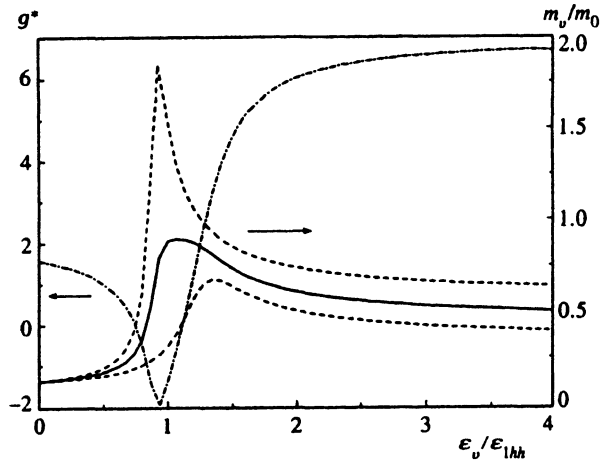


FIG. 2. Dependence of the $g$ factor (dotted line), the cyclotron mass (solid line), and the maximum and minimum mass in the plane of the well (dashed curves) on the hole energy for the first heavy-hole subband; $\varepsilon_{1hh}=(\gamma_1-2\gamma_2)(\hbar^2 2m_0)(\pi/L)^2$ is the size-quantized energy of the first heavy-hole subband in a well of width $L$.

In the opposite limiting case this scheme no longer holds: the two Landau ladders associated with the two branches of the spectrum are independent. Despite this, as before, it is convenient to assign the indices $m$ and $-m$ to them.

To conclude this section, we present some results of the numerical calculations for the first heavy-hole size-quantized subband in a rectangular quantum well based on GaAs with infinite barriers. The lack of an inversion center in GaAs was ignored (i.e., $O_hS$ symmetry was assumed). We used the wave functions and the spectrum $\varepsilon_v(k,\varphi)$ in the absence of a magnetic field that were obtained in Ref. 10 with the Luttinger parameters $\gamma_1=6.8$, $\gamma_2=1.9$, $\gamma_3=2.7$, and $\kappa=1.2$.

Figure 2 shows the plots of the energy dependence of the hole cyclotron mass

$$m_v=\frac{\hbar^2}{2\pi}\frac{dA_v}{d\varepsilon_v},$$

as well as the greatest (in the [110] direction) and smallest (in the [100] direction) effective lateral masses

$$m_v(\varphi)=\hbar^2 k\left(\frac{\partial\varepsilon_v}{\partial k}\right)^{-1}.$$

The figure also shows the hole effective $g$ factor $g^*=4\mu_v H/\hbar\omega_v$. The value of $\mu_v$ was calculated using Eqs. (6), (7), and (12), and $\omega_v\equiv eH/m_v c$.

The wave function of a conduction-band electron can be constructed in a similar manner [compare (A20)]

$$\Phi=\sum_\mu \phi_\mu w_\mu. \tag{14}$$

The expression for $\phi_\mu$ coincides with (9) when $\chi_\mu(z,\mathbf{k})$ is replaced by $\eta_\mu(z,\mathbf{k})$ and $j=3/2$ is replaced by $j=1/2$. Under the quantization conditions (13) we must replace $(-\hbar\omega)$ by $\hbar\omega$.

## 3. MATRIX ELEMENTS OF INTERBAND OPTICAL TRANSITIONS

The probability of optical transitions can be expressed in terms of the matrix elements of the operator $\hat{\mathbf{p}}\cdot\mathbf{e}$, where $\mathbf{e}$ is the light polarization vector (when the direction of the light ray is chosen normal to the plane of the quantum well, the vector $\mathbf{e}$ has the components $e_X$ and $e_Y$) and $\hat{\mathbf{p}}$ is the momentum operator, which acts only on the Bloch amplitudes. On the basis of the definitions of these amplitudes (see the Appendix), we have

$$\langle w_{\pm 1/2}|\hat{\mathbf{p}}\cdot\mathbf{e}|u_{\pm 3/2}\rangle=\frac{P}{\sqrt{2}}e_\pm,$$

$$\langle w_{\pm 1/2}|\hat{\mathbf{p}}\cdot\mathbf{e}|u_{\mp 1/2}\rangle=-\frac{P}{\sqrt{6}}e_\mp, \tag{15}$$

where $P=i\langle\mathscr{S}|\hat{p}_X|\mathscr{X}\rangle$, $e_\pm=e_X\pm ie_Y$, and the remaining matrix elements are equal to zero. Using the equations obtained above, we find

$$\langle\Psi|\hat{\mathbf{p}}\cdot\mathbf{e}|\Phi\rangle=e_+F_-+e_-F_+, \tag{16}$$

$$F_\pm=\frac{1}{\sqrt{2}}\langle P\Phi_{\mp 1/2}|\Psi_{\mp 3/2}\rangle-\frac{1}{\sqrt{6}}\langle P\Phi_{\pm 1/2}|\Psi_{\mp 1/2}\rangle. \tag{17}$$

In the overlap integrals of the electron and hole envelopes we neglect in terms that oscillate rapidly in $x$, and we take the remaining integrals over $x$ by the saddle-point method. At the saddle point $d\Delta\theta/dx=0$, where $\Delta\theta\equiv\theta_v(x)-\theta_c(x)$, and in the semiclassical approximation only the difference between the actions $\Delta s=s_v(x)-s_c(x)$ should be differentiated. (Here and in the following, the subscript $v$ refers to the valence band, and the subscript $c$ refers to the conduction band.) Then the saddle point is determined by the condition $k_{vx}=k_{cx}$, while according to (8) we have $k_{vy}=k_{cy}$ for all $x$. This means that the main contribution to the overlap integral is made by the crossing points of the trajectories of the valence-band and conduction-band electrons (Fig. 1).

Taking into account that

$$\frac{d^2s}{dx^2}=\frac{dk_x}{dx}=\lambda^{-2}\frac{dk_x}{dk_y}=-\lambda^{-2}\frac{v_y}{v_x},$$

we have

$$\frac{d^2\Delta s}{dx^2}=\frac{[\mathbf{v}_v\times\mathbf{v}_c]_z}{\lambda^2 v_{vx}v_{cx}}. \tag{18}$$

Thus,

$$F_\pm=B\sum_{l=0}^{7}\exp\left[i\Delta\theta_l+i\frac{\pi}{4}\delta_l\right]f_\pm(\mathbf{k}_l). \tag{19}$$

Here

$$f_\pm(\mathbf{k})=\int dz P\left[\frac{1}{\sqrt{2}}\eta^*_{\mp 1/2}\chi_{\mp 3/2}-\frac{1}{\sqrt{6}}\eta^*_{\pm 1/2}\chi_{\mp 1/2}\right],$$
$$B=\sqrt{\frac{\lambda^2\omega_c\omega_v}{2\pi|[\mathbf{v}_v\times\mathbf{v}_c]_z|}},\quad \delta_l=\operatorname{sgn}\left(\frac{d^2\Delta s}{dx^2}\right)_l. \tag{20}$$

The subscript $l$ indicates that the corresponding quantity must be taken at the orbit crossing point labeled $l$. The coefficient $B$ is identical for all meeting points.

In a bulk material with $O_h$ symmetry ($O_hS$ and $O_hA$ wells), according to (A7) and the analogous equations for the conduction band, we have

$$f_{\pm}(\mathbf{k}_{2p+l})=f_{\pm}(\mathbf{k}_l)\exp\left[i\frac{\pi}{2}p\Delta_{\pm}\right],$$

$$f_{\pm}(\mathbf{k}_{2p+1-l})=f_{\pm}^{*}(\mathbf{k}_l)\exp\left[i\frac{\pi}{2}(p+2)\Delta_{\pm}\right], \tag{21}$$

where $\Delta_{\pm}\equiv m_v-m_c\pm 1$. Then, it follows from Fig. 1 and the quantization conditions (13) that

$$\Delta\theta_{2p+l}=\Delta\theta_l+p\frac{2\pi\Delta n}{4},$$

$$\Delta\theta_{2p+1-l}=-\Delta\theta_l+(p+1)\frac{2\pi\Delta n}{4}, \tag{22}$$

$$\delta_l=(-1)^{l+1},$$

where $\Delta n=n_v-n_c$. Performing the summation in Eq. (19) with the use of (21) and (22), we find the selection rules $\Delta_{\pm}+\Delta n=4N$, i.e.,

$$(\pm 1+n_v+m_v)-(n_c+m_c)=4N, \quad N=0,\pm 1,\pm 2,\ldots \tag{23}$$

Here the plus sign corresponds to right-handed polarization, and the minus sign corresponds to left-handed polarization.

The left-hand side of the equality (23) can be interpreted as the change in total angular momentum during the transition (which includes the "momentum" of the electron $n+m$ and the photon $\pm 1$). The lack of conservation of angular momentum is due to warping of the orbits.

When the selection rules (23) are obeyed,

$$F_{\pm}=\exp\left[i\frac{\pi}{4}\Delta_{\pm}\right]\cdot 8B\ \mathrm{Re}\left\{f_{\pm}(\mathbf{k}_0)\right.$$
$$\left.\times\exp\left[i\Delta\theta_0-i(\Delta_{\pm}+1)\frac{\pi}{4}\right]\right\}. \tag{24}$$

The number $N$ in the selection rules (23) is restricted with semiclassical accuracy by the condition for crossing of the electron and hole orbits. This condition can be illustrated by the model used for Fig. 2 (a rectangular well in GaAs with infinite walls). The solid curve in Fig. 3 depicts the dependence of the area of the hole orbit on the hole energy. The dashed curves show the areas of the electron orbits inscribed and circumscribed around the hole orbit with the assigned energy (see the inset in Fig. 3). To determine the energy range of the holes whose orbits cross a given electron orbit, the following construction must be performed. The area (in the $\mathbf{k}$ plane) of the electron orbit $A_c=2\pi n_c\lambda^{-2}$ is determined from the number $n_c$ of the electron Landau level, and it is plotted on the $y$ axis. The segment $(\varepsilon_{v,\min},\varepsilon_{v,\max})$ marked off in Fig. 3 on the $x$ axis gives the range of hole energies sought. The range $(A_{v,\min},A_{v,\max})$ on the $y$ axis is the corresponding range of hole orbit areas, which can be used to determine the number of the hole Landau levels

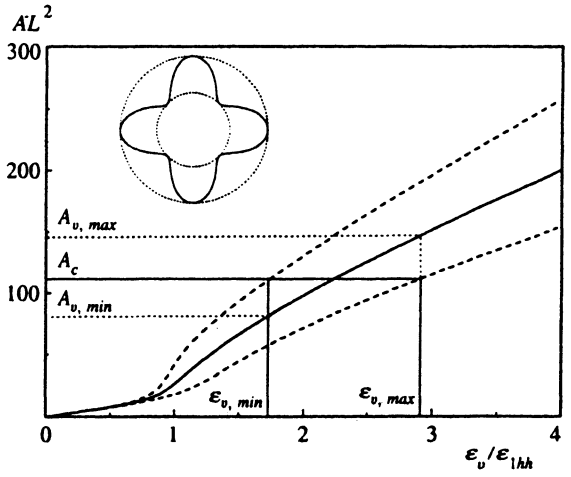


FIG. 3. Areas of orbits. Inset: limiting cases for the relative positions of the electron and hole orbits. An explanation is given in the text.

($A_{v,\min}\lambda^2/2\pi<n_v<A_{v,\max}\lambda^2/2\pi$) for which the semiclassical treatment of optical transitions performed above has meaning. We note that the relations between $A_c$ and $n_c$ and between $A_v$ and $n_v$ do not take into account the magnetic moments of the particles, which would provide only superfluous accuracy.

Equation (19) expresses the transition dipole moment as a sum of the moments of the eight dipoles corresponding to the eight crossing points of the electron and hole orbits. When the selection rules (23) are obeyed, all the dipoles with even numbers oscillate in phase (this is also true for the dipoles with odd numbers).

In the case of a symmetric quantum well, the selection rules (23) must be supplemented by a restriction associated with the symmetry under the reflection $\hat{\Pi}_z$: only transitions between states with identical symmetry are allowed. [Otherwise, according to (A9), the integrand in Eq. (20) is an odd function of $z$, and $f_{\pm}(\mathbf{k})=0$.]Then (A11) yields the relation

$$f_{\pm}^{-m_c,-m_v}=-(f_{\mp}^{m_c,m_v})^{*}. \tag{25}$$

Let us now move on to the case of $T_dS$ symmetry. Here we must use the operators $\tilde{Q}_n^{(m)}$ instead of $\hat{Q}_n^{(m)}$, as well as the relations (A17) instead of (A7). However, Eqs. (21) are retained, so that the selection rules (23) and the expressions (24) for the transition matrix elements are also retained.

The situation changes significantly in the case of $T_dA$ symmetry. Here we have the symmetry not of a square, but of a rectangle oriented along the [110] axis. There are no symmetry relations like (A2) that would express the wave function in all sectors of the $\mathbf{k}$ plane in terms of its values in one of the sectors. However, there is such a relation between sectors *0*, *3*, *4*, and *7*, as well as between sectors *1*, *2*, *5*, and *6*. Summing in Eq. (19) with the use of the permissible (with consideration of these restrictions) relations from (21) and (22), we obtain the selection rules

$$(\pm 1+n_v+m_v)-(n_c+m_c)=2N. \tag{26}$$

Here

$$F_{\pm}=\exp\left(i\frac{\pi}{4}\Delta_{\pm}\right)4B\ \mathrm{Re}\left\{f_{\pm}(\mathbf{k}_0)\exp\left[i\Delta\theta_0-i(\Delta_{\pm}+1)\frac{\pi}{4}\right]\right.$$

$$\left.+f_{\pm}(\mathbf{k}_1)\exp\left[i\Delta\theta_1-i(\Delta_{\pm}-1)\frac{\pi}{4}\right]\right\}. \quad (27)$$

It is seen that the selection rules (26) actually do not depend on the sign of the circular light polarization.

Finally, let us consider the cylindrical approximation. In this approximation the orbits of both the conduction-band and valence-band electrons are circles. The radii of these circles must be close (in accordance with the condition $\Delta n \ll n_v, n_c$); otherwise, the overlap integral in (17) will be small. It follows from the quantization conditions (13) and cylindrical symmetry that

$$\Delta\theta(x)=\frac{\tilde{\varphi}(x)}{2\pi}\cdot 2\pi\Delta n, \quad (28)$$

where $\tilde{\varphi}(x)$ is the angle between the radius vectors of electrons at the points $x$ and $a$, and $\tilde{\varphi}(x)=\varphi+\pi/4$. The dependence of the envelopes $\chi_\mu(z,\mathbf{k})$ on the angle $\varphi$ is given by Eq. (A13), whence

$$f_{\pm}(\mathbf{k})=f_{\pm}(\mathbf{k})|_{\varphi=-\pi/2}\cdot\ \exp[i\Delta_{\pm}(\varphi+\pi/2)]. \quad (29)$$

The overlap integral in (17) can be calculated by transforming from integration over $x$ to integration over $\tilde{\varphi}$ and utilizing the fact that

$$d\tilde{\varphi}=\frac{\omega_c}{|v_{cx}|}dx=\frac{\omega_v}{|v_{vx}|}dx=\sqrt{\frac{\omega_v\omega_c}{|v_{vx}v_{cx}|}}dx.$$

As a result we obtain the selection rules (23), but we must set $N=0$ in them, which corresponds to conservation of the total angular momentum during the transition. Under these conditions

$$F_{\pm}=\exp\left(i\frac{\pi}{4}\Delta_{\pm}\right)f_{\pm}(\mathbf{k})|_{\varphi=-\pi/2}. \quad (30)$$

The selection rules obtained above are presented in Fig. 4 for transitions between the first exciton size-quantized subband and the first heavy-hole subband. The solid lines depict transitions that are allowed in a symmetric well in the cylindrical approximation ($CS$ symmetry). Transitions with a change in the Landau-level number by 2 are caused by the mixing of heavy- and light-hole states and are of low intensity when the hole kinetic energies are small (compared with the size-quantized energy).

Under $O_hS$ symmetry (i.e., with consideration of the warping of the valence band), besides the transitions indicated, transitions with a $n_v \to n_v+4N$ shift, which are not depicted in Fig. 4, become possible. Consideration of the $T_d$ symmetry of the bulk material (rather than $O_h$) or the asymmetry of the quantum well makes the transitions represented by the dashed lines in Fig. 4 possible (with a possible $n_v \to n_v+4N$ shift).

The same scheme of selection rules is also maintained for transitions between electron and heavy-hole size-quantized subbands with numbers of identical parity ($1hh-3e$, $2hh-2e$, ...).

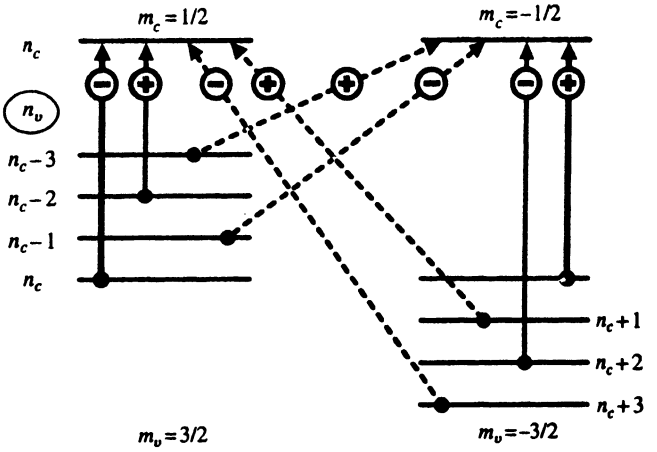


FIG. 4. Transitions between the first heavy-hole size-quantized subband and the first electron subband. The Landau level $n_c$ in the conduction band is fixed. Only the Landau levels $n_v$ in the valence band from which a transition is possible to the $n_c$ level under cylindrical symmetry are shown. The arrangement of the right-hand Landau ladder relative to the left-hand ladder (along the energy axis) is schematic, and in reality is shifted due to the presence of a magnetic moment and the possible splitting of the two branches of the spectrum in the absence of a magnetic field.

If the subbands of the electrons and heavy holes participating in a transition have different parities, the scheme described above changes. Under $O_hS$ or $CS$ symmetry the transitions represented in Fig. 4 by dashed lines are allowed, and lowering the symmetry makes the transitions represented by the solid lines possible. It is noteworthy, however, that in this case the optical transitions in a symmetric well always result from the mixing of heavy- and light-hole states, and therefore their intensity is low when the hole kinetic energies are low.

Simultaneous consideration of the lack of an inversion center in the bulk material and the asymmetry of the quantum well ($T_dA$ symmetry) leads to the appearance of an additional axis in the plane of the well. In this case all the transitions noted in Fig. 4 are possible in both polarizations, i.e., they are elliptically polarized.

Transitions between electron and light-hole subbands can be treated similarly.

To illustrate this, Fig. 5 presents an example of a calculation of the possible transitions in the model used for Figs. 2 and 3. The curves 8–16 numbered give the energies of the hole Landau levels with the respective numbers as a function of the magnetic field. The hole levels that can participate in transitions to the electron level having $n_c=10$ with plus polarization are depicted. The solid portions of the curves correspond to orbits that cross the particular electron orbit.

Horizontal segments are shown at three values of the magnetic field. Their lengths are proportional to the square of the absolute value of the transition matrix element $|F_+|^2$ [calculated from Eq. (24)]. We note that the intensity of a transition is proportional to $|F_+|^2/\lambda^2$.

The intensity has some special features when the electron and hole orbits touch one another (see the inset in Fig. 3). In this case the vector product in the denominator of the expression for $B$ in (22) vanishes. These features are similar to those found by Portnoĭ[11] for the distribution function of

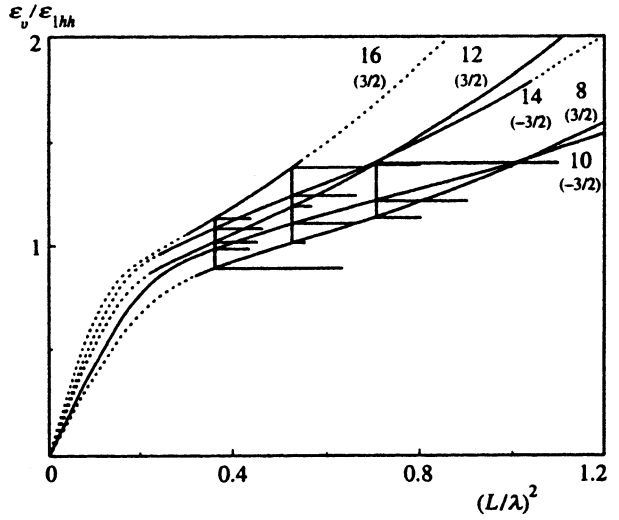


FIG. 5. Energy of the hole Landau levels participating in transitions to the electron level $n_c=10$ with "plus" polarization. An explanation is given in the text.

photoexcited electrons in a quantum well without a magnetic field.

Thus, the selection rules and expressions for the matrix elements of interband optical transitions in a quantum well in a magnetic field have been obtained in this work. The warping and complex structure of the valence band have been taken into account. The matrix elements in the semiclassical approximation have been expressed in terms of the wave functions of the electrons and holes in the absence of a magnetic field. It has been shown that in this approximation the intensity of a transition can be regarded as resulting from interference of the fields of the eight dipoles corresponding to the crossing points of the electron and warped hole orbits.

We thank I. A. Merkulov for useful discussions.

This work was supported by the Russian Fund for Fundamental Research (Project 95-02-04055), as well as the International Science Foundation (Grant R47300).

## APPENDIX A: WAVE FUNCTIONS IN A WELL WITHOUT A MAGNETIC FIELD

Let us first consider a symmetric well with $O_h$ symmetry for the bulk material (an $O_hS$ well). It is assumed that the well points in the [001] direction (the $z$ axis). The $X$ and $Y$ axes are directed along the [100] and [010] crystal axes in the plane of the well. We write the wave function of a valence-band electron in the form

$$\Psi_{\mathbf{k}}=\exp(i\mathbf{k}\rho)\sum_{\mu}\chi_{\mu}^{(m)}(z,\mathbf{k})u_{\mu}, \tag{A1}$$

where $\mathbf{k}$ is the wave vector in the plane of the well, the $u_\mu$ are the Bloch amplitudes corresponding to angular momentum $j=3/2$ and projection of the angular momentum onto the $z$ axis $\mu=\pm 3/2,\pm 1/2$. The superscript $m$ has the following meaning: when $\mathbf{k}\to 0$, only one term with $\mu=m$ remains in the sum (A1) in the case of $O_hS$ symmetry under consideration. Thus, $m$ is the projection of the angular momentum onto the $z$ axis when $\mathbf{k}\to 0$. It is customary to use the value of $|m|$ to distinguish between the size-quantized subbands. The subbands with $m=\pm 1/2$ are usually called light-hole subbands, and those with $m=\pm 3/2$ are called heavy-hole subbands. In an $O_hS$ well the $\pm m$ states are degenerate for all $\mathbf{k}$.

The $\mathbf{k}$ plane can be divided into eight sectors (Fig. 1). If $\Psi_{\mathbf{k}}$ is assigned for sector *1*, its values for all the remaining sectors can be found to within a constant phase factor (which may depend on $\mathbf{k}$) from symmetry arguments. This can be accomplished by successively applying the operators $\hat{K}$, $\hat{\Pi}_X$, and $\hat{R}$, which commute with the Hamiltonian. Here $\hat{K}$ is the time-inversion operator, $\hat{\Pi}_X$ causes reflection in the $YZ$ plane, and $\hat{R}$ effects rotation through $\pi/2$ about the $z$ axis. These operators are defined in the following manner:[12]

$$\hat{K}\Psi=-i\hat{\sigma}_y\Psi^*,\quad \hat{\Pi}_X\Psi(\mathbf{r})=\hat{\sigma}_x\Psi(\Pi_X\mathbf{r}),$$

$$\hat{R}\Psi(\mathbf{r})=\exp(-i\hat{J}_z\pi/2)\Psi(\mathbf{r})$$
$$=\exp(-i\hat{\sigma}_z\pi/4)\Psi(R^{-1}\mathbf{r}).$$

Here the $\hat{\sigma}_\alpha$ are Pauli matrices, and $\Pi_X$ and $R$, acting on a radius vector with the components $(X,Y,z)$, transfer it to $(-X,Y,z)$ and $(-Y,X,z)$, respectively. At the same time, the operators $\hat{K}$, $\hat{\Pi}_X$, and $\hat{R}$ do not alter $m$; therefore their application yields a state belonging to the same branch of the size-quantized subband. If $\mathbf{k}$ lies in sector *1*, we can specify the wave functions in the sector with the number $m$ by the equality

$$\Psi_{Q_n\mathbf{k}}^{(m)}=\hat{Q}_n^{(m)}\Psi_{\mathbf{k}}^{(m)}. \tag{A2}$$

Here the operators $Q_n$ act in the $\mathbf{k}$ plane and translate the vector $\mathbf{k}$ to equivalent points on the $\mathbf{k}$ plane (see Fig. 1):

$$Q_{2p}=\Pi_X R^{2-p},\quad Q_{2p+1}=R^p,\quad p=0,1,2,3, \tag{A3}$$

where $\Pi_X$ and $R$ denote reflection and rotation in the $\mathbf{k}$ plane. If we use $\varphi$ to denote the angle between the vector $\mathbf{k}$ and the $X$ axis, $Q_{2p+1}$ translates $\varphi$ to $\varphi+p\pi/2$, and $Q_{2p}$ translates $\varphi$ to $p\pi/2-\varphi$.

The operations (A3) form the group of a square. We define the operators $\hat{Q}_n^{(m)}$ in the following manner:

$$\hat{Q}_{2p}^{(m)}=(-1)^{j+m}\exp(imp\pi/2)\hat{K}\hat{\Pi}_X\hat{R}^{4-p},$$

$$\hat{Q}_{2p+1}^{(m)}=\exp(imp\pi/2)\hat{R}^p. \tag{A4}$$

It is easy to verify that the operators $\hat{Q}_n^{(m)}$ do, in fact, translate $\Psi_{\mathbf{k}}^{(m)}$ into $\Psi_{Q_n\mathbf{k}}^{(m)}$, and the equality (A2) indicates a definite choice of phases in sector $n$ relative to sector 1. The phase factors in (A4) were chosen such that the operators (A4) form a group that is isomorphic to the group of a square (A3) for any half-integer $j$ and $m$. Thus, the equality (A2) is valid for any $\mathbf{k}$ and not just for $\mathbf{k}$ from sector *1*.

Let us dwell on the question of why the operators $\hat{Q}_n^{(m)}$ in (A2) were chosen to be different for different values of $m$. In principle, the phases of the functions $\Psi_{\mathbf{k}}^{(m)}$ in different sectors could have been determined from (A2) using the operators $\hat{Q}_n^{(m_0)}$ with any fixed half-integer value of $m_0$ that does not depend on $m$. However, it is natural that when

$\mathbf{k}\to 0$, the function $\Psi_{\mathbf{k}}^{(m)}$ should not depend on the direction of $\mathbf{k}$. The phases in (A4) were chosen so as to be compatible with this requirement.

We choose the phases of the Bloch amplitudes according to Ref. 13:

$$u_{\pm 3/2}=\mp\frac{1}{\sqrt{2}}(\mathscr{X}\pm i\mathscr{Y})\nu_{\pm},$$

$$u_{\pm 1/2}=\frac{1}{\sqrt{6}}[\mp(\mathscr{X}\pm i\mathscr{Y})\nu_{\mp}+2\mathscr{Z}\nu_{\pm}], \tag{A5}$$

where the $\nu_{\pm}$ are spin functions with a spin projection onto the $z$ axis equal to $\pm 1/2$. Then

$$\hat{K}u_{\mu}=(-1)^{j+\mu}u_{-\mu},\quad \hat{\Pi}_X u_{\mu}=u_{-\mu},$$
$$\hat{\Pi}_z u_{\mu}=(-1)^{j-\mu}u_{\mu},\quad \hat{R}u_{\mu}=\exp(-i\mu\pi/2)u_{\mu}. \tag{A6}$$

Using (A2), (A4), and (A6), for the envelopes we can find

$$\chi_{\mu}^{(m)}(z,Q_{2p}\mathbf{k})=\exp[(m-\mu)(p+2)\pi/2]\chi_{\mu}^{(m)*}(z,\mathbf{k}),$$
$$\chi_{\mu}^{(m)}(z,Q_{2p+1}\mathbf{k})=\exp[(m-\mu)p\pi/2]\chi_{\mu}^{(m)}(z,\mathbf{k}). \tag{A7}$$

It is seen from (A7), in particular, that the envelope $\chi_{\mu}^{(m)}$ with $\mu=m$ (which remains as the only nonzero envelope when $\mathbf{k}\to 0$) is not altered by the transformations $\hat{Q}_n^{(m)}$.

The uniqueness of the wave functions requires that both Eqs. (A7) yield identical results on the sector boundaries. This means that

$$\chi_{\mu}^{(m)}(z,\mathbf{k})=(-1)^{m-\mu}\chi_{\mu}^{(m)*}(z,\mathbf{k}) \text{ for } \varphi=0, \tag{A8a}$$

$$\chi_{\mu}^{(m)}(z,\mathbf{k})=\exp[i(\mu-m)\pi/2]\chi_{\mu}^{(m)*}(z,\mathbf{k}) \text{ for } \varphi=\frac{\pi}{4}. \tag{A8b}$$

It can be assumed that a state with given $m$ has definite (independent of the number of the size-quantized subband) symmetry with respect to the reflection operation $\hat{\Pi}_z$, i.e., either $\hat{\Pi}_z\Psi_{\mathbf{k}}^{(m)}=\Psi_{\mathbf{k}}^{(m)}$ or $\hat{\Pi}_z\Psi_{\mathbf{k}}^{(m)}=-\Psi_{\mathbf{k}}^{(m)}$. (The operator $\hat{\Pi}_z$ commutes with the Hamiltonian and with the operators $\hat{Q}_n^{(m)}$.) Hence it follows for the envelopes that

$$\chi_{\mu}^{(m)}(-z,\mathbf{k})=\pm(-1)^{j-\mu}\chi_{\mu}^{(m)}(z,\mathbf{k}). \tag{A9}$$

The plus sign corresponds to the case in which the state is symmetric for the particular value of $m$, and the minus sign corresponds to the case in which it is antisymmetric.

States with opposite values of $m$ have opposite symmetry. If the state $\Psi_{\mathbf{k}}^{(m)}$ is symmetric, $\Psi_{\mathbf{k}}^{(-m)}$ is antisymmetric. The latter state can be obtained from the former by applying the operator $\hat{K}\hat{I}$, where $\hat{I}$ is spatial inversion. In fact, $\hat{K}\hat{I}$ anticommutes with $\hat{\Pi}_z$ and therefore alters the symmetry. It can be assumed for the symmetric state $\Psi_{\mathbf{k}}^{(m)}$ that

$$\Psi_{\mathbf{k}}^{(-m)}=\hat{K}\hat{I}\Psi_{\mathbf{k}}^{(m)}. \tag{A10}$$

It follows from this equation and (A9) that

$$\chi_{\mu}^{(-m)}(z,\mathbf{k})=(-1)^{j+1/2}\chi_{-\mu}^{(m)*}(z,\mathbf{k}). \tag{A11}$$

The relation (A10) must be compatible with the transformation rules (A2). This requires that

$$\hat{K}\hat{Q}_n^{(m)}\hat{K}^{-1}=\hat{Q}_n^{(-m)}. \tag{A12}$$

It can be shown that this relation does, in fact, hold for the operators (A4).

The cylindrical (or spherical) approximation is often used. In this case the Hamiltonian is assumed to commute with the operator $\hat{R}_{\varphi}=\exp(-i\hat{J}_z\varphi)$ for rotation through an arbitrary angle $\varphi$. We define $\hat{R}_{\varphi}^{(m)}$ by means of the relation $\hat{R}_{\varphi}^{(m)}=\exp(im\varphi)\hat{R}_{\varphi}$. Then, if the function $\Psi_{\mathbf{k}}^{(m)}$ is specified at $\varphi=0$, it can be obtained at all $\varphi$ using the operator $\hat{R}_{\varphi}^{(m)}$: $\Psi_{\mathbf{k}}^{(m)}=\hat{R}_{\varphi}^{(m)}(\Psi_{\mathbf{k}}^{(m)}|_{\varphi=0})$, whence

$$\chi_{\mu}^{(m)}(z,\mathbf{k})=\exp[i(m-\mu)(\varphi+\pi/2)]\chi_{\mu}^{(m)}(z,\mathbf{k})|_{\varphi=-\pi/2}. \tag{A13}$$

The symmetry under the reflection $Q_4$ (which leaves the straight line $\varphi=-\pi/2$ in $\mathbf{k}$ space in place) shows that $\chi_{\mu}^{(m)}|_{\varphi=-\pi/2}$ is a real quantity. We note that (A13) satisfies the relations (A7). Equations (A9)–(A11) hold, of course, if the well is symmetric.

We have hitherto considered $O_hS$ (or $CS$) symmetry. We now move on to the case of an asymmetric well when the bulk material has $O_h$ symmetry (an $O_hA$ well). In this case two branches of the spectrum assigned to one size-quantized subband are nondegenerate when $\mathbf{k}\neq 0$. When $\mathbf{k}\to 0$, they become degenerate, but they turn into linear combinations of states with $m$ and $-m$, rather than into states with a definite angular momentum $m$. Nevertheless, it is convenient to transform the states of one of these branches using the operators $\hat{Q}_n^{(m)}$ and the states of the other branch using $\hat{Q}_n^{(-m)}$ and to denote the corresponding wave functions by $\Psi_{\mathbf{k}}^{(m)}$ and $\Psi_{\mathbf{k}}^{(-m)}$. [We reiterate that the sign of $m$ no longer has the same meaning that it had in the case of $O_hS$ symmetry, although, as before, $|m|$ indicates whether the states belong to a heavy-hole subband ($|m|=3/2$) or to a light-hole subband ($|m|=1/2$).] Then Eqs. (A2)–(A8) remain valid, but (A9)–(A11), of course, do not hold. Equation (A13) continues to be valid for $CA$ symmetry.

The operators that commute with the Hamiltonian include $\hat{K}\hat{R}^2$, which leaves the wave vector $\mathbf{k}$ unchanged. Since the states are nondegenerate in the case under consideration, $\hat{K}\hat{R}^2\Psi_{\mathbf{k}}^{(m)}$ can differ from $\Psi_{\mathbf{k}}^{(m)}$ only by a phase factor:

$$\hat{K}\hat{R}^2\Psi_{\mathbf{k}}=\exp(i\gamma_{\mathbf{k}})\Psi_{\mathbf{k}}. \tag{A14}$$

Hence it follows for the envelopes that

$$\chi_{-\mu}^{*}=\exp(ij\pi+i\gamma_{\mathbf{k}})\chi_{\mu}. \tag{A15}$$

The phase $\gamma_{\mathbf{k}}$ depends on the choice of overall phase factor of the wave function.

In the case of $T_d$ symmetry for the bulk material in a symmetric well ($T_dS$ symmetry), instead of the rotation $\hat{R}$, the rotation–reflection operator $\hat{\Pi}_z\hat{R}$ commutes with the Hamiltonian, and instead of the reflection $\hat{\Pi}_X$, $\hat{\Pi}_X\hat{R}$ commutes with the Hamiltonian. Therefore, instead of the operators (A4), we can introduce the operators $\tilde{Q}_n^{(m)}$:

$$\tilde{Q}_{2p}^{(m)}=(-1)^{j+m}\exp(imp\pi/2)\hat{K}\hat{\Pi}_X\hat{R}(\hat{\Pi}_z\hat{R})^{3-p},$$
$$\tilde{Q}_{2p+1}^{(m)}=\exp(imp\pi/2)(\hat{\Pi}_z\hat{R})^{p}. \tag{A16}$$

These operators [like the operators (A4)] form a group that is isomorphic to the group of a square (A3) and satisfy a relation that is analogous to (A12).

The following relations now follow from the equality $\Psi^{(m)}_{Q_n\mathbf{k}}=\tilde{Q}^{(m)}_n\Psi^{(m)}_{\mathbf{k}}$ instead of Eqs. (A7) and (A8a) [Eq. (A8b) remains valid]:

$$\chi^{(m)}_\mu(z,Q_{2p}\mathbf{k})=(-1)^{(p+1)(j-\mu)}\exp[(m-\mu)(p+2)\pi/2]\times\chi^{(m)*}_\mu((-1)^{p+1}z,\mathbf{k}), \tag{A17}$$

$$\chi^{(m)}_\mu(z,Q_{2p+1}\mathbf{k})=(-1)^{p(j-\mu)}\times\exp[(m-\mu)p\pi/2]\chi^{(m)}_\mu(z,\mathbf{k}), \tag{A18}$$

$$\chi^{(m)}_\mu(z,\mathbf{k})=(-1)^{j-m}\chi^{(m)*}_\mu(-z,\mathbf{k}) \quad \text{for } \varphi=0. \tag{A19}$$

The equalities (A14) and (A15) also remain valid for this type of symmetry.

The case of an asymmetric well with $T_d$ symmetry for the bulk material ($T_dA$ symmetry) requires special consideration. Here we no longer have the symmetry of a square, but the symmetry of a rectangle, in the $\mathbf{k}$ plane. The corresponding group consists of the operations $Q_1$, $Q_2$, $Q_5$, and $Q_6$, which are defined by Eqs. (A3). Accordingly, the wave functions transform according to (A2) when $n=1$, 2, 5, and 6. We note that for such $n$ we have $\tilde{Q}^{(m)}_n=\hat{Q}^{(m)}_n$ and Eqs. (A7) and (A17) coincide. The boundary conditions for $\varphi=\pi/4$ [Eq. (A8b)] remain valid, but there are no boundary conditions for $\varphi=0$.

The wave function of the conduction-band electrons can be written in a form similar to (A1):

$$\Phi^{(m)}_{\mathbf{k}}=\exp(i\mathbf{k}\rho)\sum_\mu \eta^{(m)}_\mu(z,\mathbf{k})w_\mu, \tag{A20}$$

where $\mu=\pm 1/2$, $m=\pm 1/2$, $w_\mu=i\mathscr{T}v_\mu$. Here Eqs. (A6) remain valid after the formal replacement of $u_\mu$ by $w_\mu$ and $j=3/2$ by $j=1/2$. All the remaining relations follow from them and therefore remain valid after the replacement of $\Psi_{\mathbf{k}}$ by $\Phi_{\mathbf{k}}$, $\chi_\mu$ by $\eta_\mu$, and $j=3/2$ by $j=1/2$.

We note that Eqs. (A6) must be modified for a split valence band.

[1)]Yu. N. Shlyakhter, Diploma Thesis, St. Petersburg State Technical University, 1993.


[1] *Landau Level Spectroscopy (Modern Problems in Condensed Matter Sciences, Vol. 27-2)*, G. Landwehr and E. I. Rashba (eds.) (North-Holland, Amsterdam, 1991), p. 1.
[2] H. Chu and Y.-C. Chang, Phys. Rev. B **40**, 5497 (1989).
[3] L. J. Sham, in *High Magnetic Fields in Semiconductor Physics II (Springer Series in Solid-State Physics, Vol. 87)*, (Springer-Verlag, Berlin–Heidelberg, 1989), p. 232.
[4] U. Bockelmann and G. Bastard, Phys. Rev. B **45**, 1700 (1992).
[5] S.-R. E. Yang, D. A. Broido, and L. J. Sham, Phys. Rev. B **32**, 6630 (1985).
[6] C. R. Pidgeon and R. N. Brown, Phys. Rev. **146**, 575 (1966).
[7] B. M. Gorbovitskiĭ and V. I. Perel', Zh. Éksp. Teor. Fiz. **85**, 1812 (1983) [Sov. Phys. JETP **58**, 1054 (1983)].
[8] V. M. Babich and V. S. Buldyrov, *Asymptotic Methods in Short-Wave Diffraction Problems* [in Russian] (Nauka, Moscow, 1972, p. 69).
[9] L. D. Landau and E. M. Lifshitz, *Quantum Mechanics: Non-Relativistic Theory*, 3rd ed. (Pergamon Press, Oxford, 1977) [Russ. original, 4th ed., Nauka, Moscow, 1989, p. 211].
[10] I. A. Merkulov, V. I. Perel', and M. E. Portnoĭ, Zh. Éksp. Teor. Fiz. **99**, 1202 (1991) [Sov. Phys. JETP **72**, 669 (1991)].
[11] M. E. Portnoĭ, Fiz. Tekh. Poluprovodn. **25**, 2150 (1991) [Sov. Phys. Semicond. **25**, 1294 (1991)].
[12] C. Kittel, *Quantum Theory of Solids* (Wiley, New York, 1963)
[13] A. R. Edmonds, *Angular Momentum in Quantum Mechanics* (Princeton University Press, Princeton, N.J., 1957)


Translated by P. Shelnitz